JMEPEG (2011) 20:422–435
DOI: 10.1007/s11665-010-9691-4

1059-9495/$19.00

Corrosion Behavior of Surface-Treated Implant Ti-6Al-4V by Electrochemical Polarization and Impedance Studies

Subir Paul and Kasturi Yadav

(Submitted September 17, 2009; in revised form May 4, 2010)

Implant materials for orthopedic and heart surgical services demand a better corrosion resistance material than the presently used titanium alloys, where protective oxide layer breaks down on a prolonged stay in aqueous physiological human body, giving rise to localized corrosion of pitting, crevice, and fretting corrosion. A few surface treatments on Ti alloy, in the form of anodization, passivation, and thermal oxidation, followed by soaking in Hank solution have been found to be very effective in bringing down the corrosion rate as well as producing high corrosion resistance surface film as reflected from electrochemical polarization, cyclic polarization, and Electrochemical Impedance Spectroscopy (EIS) studies. The XRD study revealed the presence of various types of oxides along with anatase and rutile on the surface, giving rise to high corrosion resistance film. While surface treatment of passivation and thermal oxidation could reduce the corrosion rate by 1/5th, anodization in 0.3 M phosphoric acid at 16 V versus stainless steel cathode drastically brought down the corrosion rate by less than ten times. The mechanism of corrosion behavior and formation of different surface films is better understood from the determination of EIS parameters derived from the best-fit equivalent circuit.

Keywords biomaterials, coatings, corrosion testing, titanium

1. Introduction

Titanium and its alloys, depending on its grade, have high tensile strength, fracture toughness, excellent corrosion resistance, biocompatibility, and osseo-integration behavior, and hence are useful for various implant applications. The stability of titanium under corrosive environment is essentially due to the formation of a stable and tightly adherent thin protective oxide layer or passive film on its surface. In general, it is known that titanium metal is spontaneously covered by a surface oxide of 1.5-10 nm thickness, (Ref 1). The outer covering oxide of a titanium implant consists mainly of TiO_2 (Ref 2, 3), and is basically amorphous in crystal structure and morphologically homogeneous (Ref 4). Moreover, this thin oxide surface layer results in an excellent resistance to corrosion indicated by a low level of electronic conductivity (Ref 5), thermodynamically great stability (Ref 6, 7), and low ion-formation tendency in aqueous environments (Ref 8). These properties of the natural oxide layer may be the reasons for the excellent biocompatibility leading to favorable tissue responses to titanium implants in comparison to many other metal implants (Ref 9). de Assis et al. (Ref 10) studied the corrosion characteristics of titanium alloys by electrochemical techniques and found very low current densities, indicating a typical passive behavior for all investigated alloys However, during the prolonged use of this implant in orthopedic and heart surgery applications, the passive film is found to become unstable in aqueous human physiological environment, giving rise to localized corrosion of pitting and crevice, which further cause chemical-biological interactions, tissue discoloration, and allergic reactions in patients.

Efforts are being made to make Ti and its alloys better corrosion resistant by surface treatments. Narayanan and Seshadri (Ref 11), in their investigation of anodization of Ti-6Al-4V from phosphoric acid electrolyte to form coatings, showed very good resistance to the attack by this medium. Wong et al. (Ref 12) could form a potentially bioactive, and at the same time, corrosion-resistant surface layer on NiTi by AC anodization, followed by hydrothermal treatment. Narayanan and Seshadri (Ref 13) made multiple coatings on Ti-6Al-4V by electrochemical and hydrothermal treatments, tested in simulated body fluid, and reported to have obtained maximum corrosion resistance with layers of oxide, followed by hydroxyapatite.

In this investigation, attempts have been made to produce an implant material with very high resistance to localized corrosion by forming protective surface films by three different surface treatments, namely, anodization in phosphoric acid, prolong passivation in Hank solution, and thermal oxidation followed by soaking in SBF. Electrochemical characterization of alloy Ti-6Al-4V has been extensively carried out by potentiodynamic polarizations, cyclic polarizations, and electrochemical impedance spectrometry. XRD studies have also been carried out to characterize the structure and phases.

2. Experimental Procedure

The test specimen was hot rolled, in the form of rod of 6-mm diameter. The sharp edges, dirt, any oxide layer, and rough surfaces were removed by grinding. The samples were

Subir Paul and **Kasturi Yadav**, Department of Metallurgical and Material Engineering, Jadavpur University, Kolkata 700032, India. Contact e-mail: spaulxx@ymail.com.

heat treated by annealing at a temperature of 800 °C in argon atmosphere. Manual metallographic grinding procedure was performed up to the 3/0 emery paper and then polished on polishing wheel. The samples were then rinsed by water and subsequently by ethanol.

2.1 Corrosion Testing

Standard Corrosion Cell has been used to perform the electrochemical potentiostatic polarization tests on the specimen. Experiments have been carried out as per standard methods (Ref 14-18), using Gamry Potentiostat. All the experiments were performed in Hank solution, whose composition is depicted in Table 9. A pH of 7.4 and human body temperature of 37 °C were maintained throughout the experiment. Corrosion rates were determined by Linear polarization as well as Tafel extrapolation methods. Then, cyclic polarization experiment is done with the sample in the similar way. A series of experimentation of AC Electrochemical impedance spectroscopy (EIS) was carried out in Gamry instrument to get Nquist and Bode plots. EIS parameters were computed using Gamry software. All the experiments were repeated for at least 2 times to confirm the consistency of the experimental data.

Table 1 E_{corr} and I_{corr} values of untreated Ti-6Al-4V and 316L stainless steel

Sample	E_{corr}, mV vs. SCE	I_{corr}, μA/cm^2
Stainless steel 316L	−466.0	5.767
Titanium alloy	−97.09	4.225

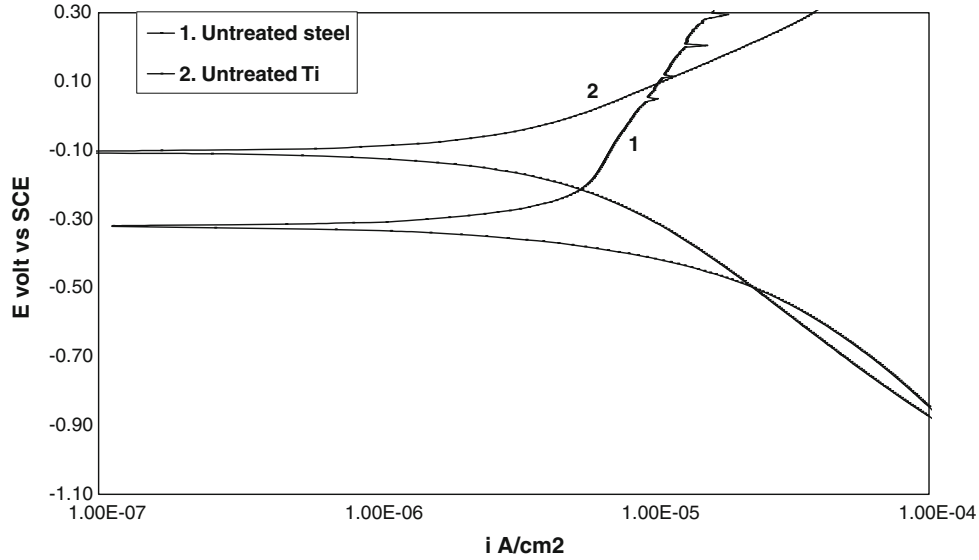

Fig. 1 Comparison of potentiodynamic curves of 316L steel and Ti-6Al-4V

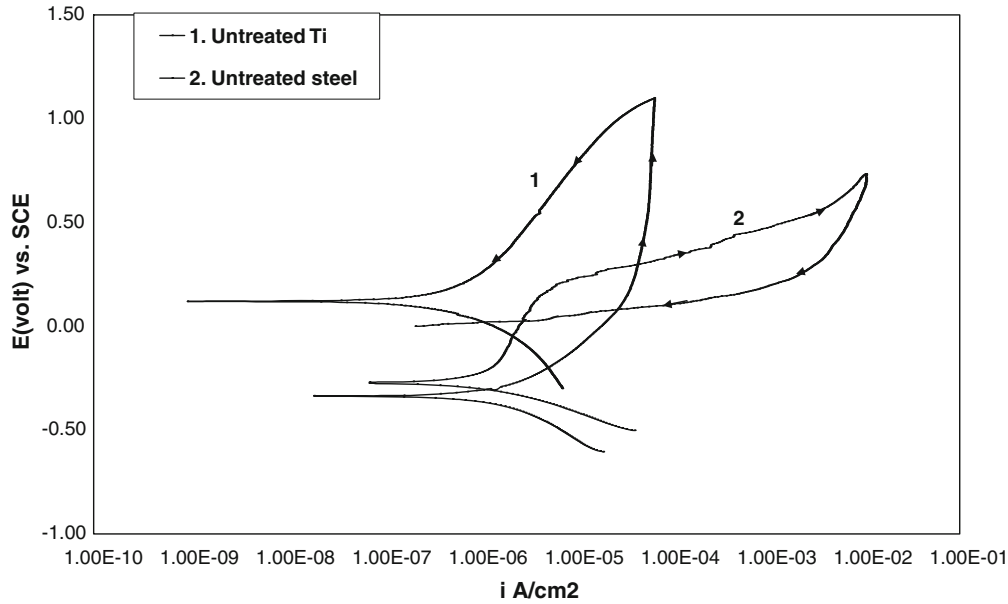

Fig. 2 Comparison of cyclic polarization curves of 316L steel and Ti-6Al-4V

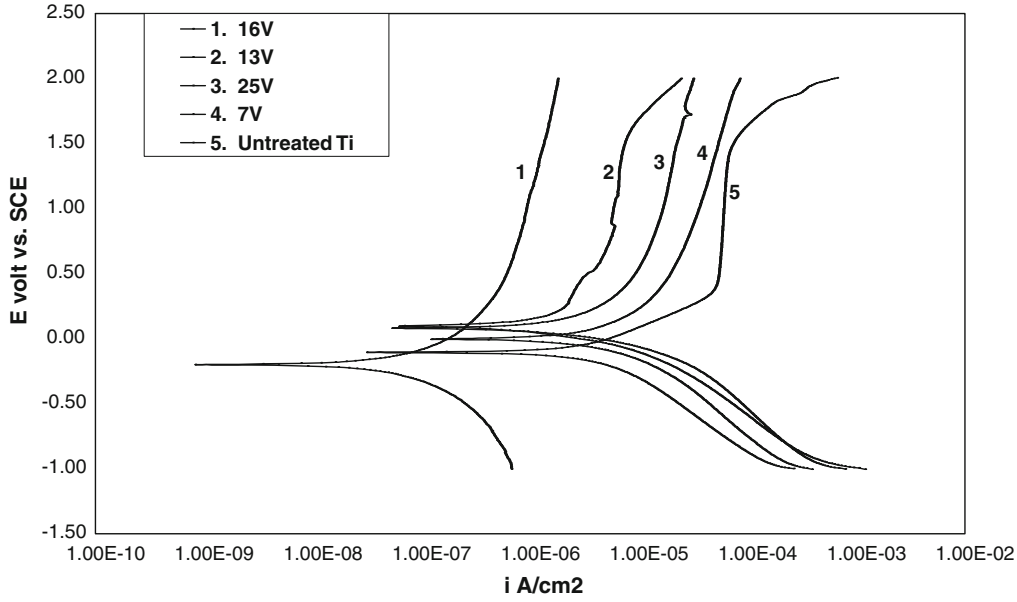

Fig. 3 Potentiodynamic curves of Ti alloy in Hank solution after surface treatment of anodization in phosphoric acid for 30 min at different potentials

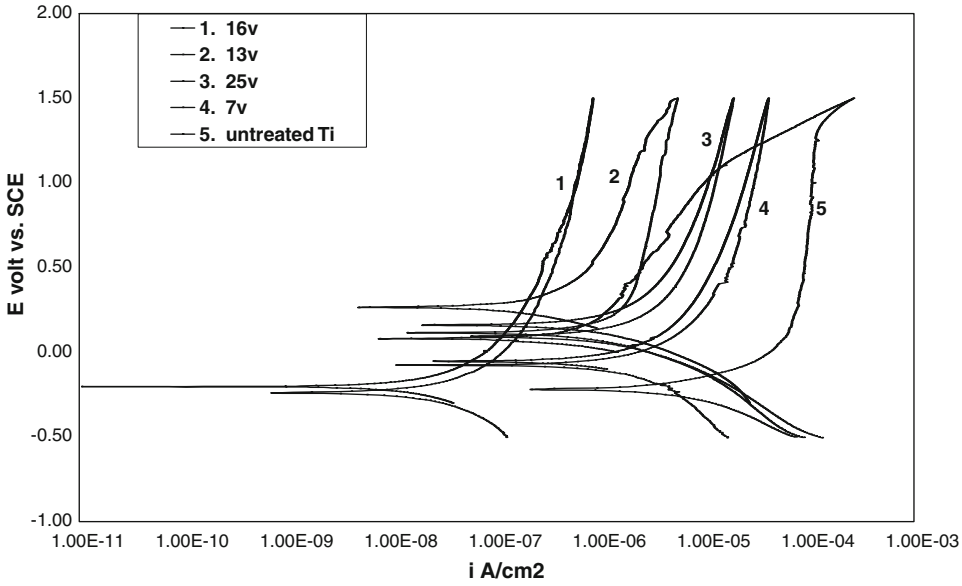

Fig. 4 Cyclic polarization curves of Ti alloy in Hank solution after surface treatment of anodization in 0.3 M phosphoric acid for 30 min at different potentials

Table 2 E_{corr} and I_{corr} values of Ti alloy in Hank solution after surface treatment by anodization in 0.3 M phosphoric acid

Sample	E_{corr}, mV vs. SCE	I_{corr}, μA/cm^2
7 V 30 min	−11.63	3.819
13 V 30 min	125.0	1.319
16 V 30 min	−203.5	0.051
25 V 30 min	82.85	1.802

2.2 Surface Modification Treatments

2.2.1 Anodization. Polished samples were anodized in 0.3 M phosphoric acid, against 304 stainless steel cathode. A magnetic stirrer was taken for constant stirring, and the temperature was maintained at 25 ± 1 °C. The samples were anodized at 7, 13, 16, and 25 V, with respect to the cathode.

2.2.2 Passivation. Passivation was carried out by potentiostatic method, where the polarized sample is passivated at a preselected potential below the breakdown potential, determined from the potentiodynamic polarization curve.

Samples were passivated potentiostatically by immersing in Hank solution at various preselected potentials of 0.5, 1, and 1.2 V, versus SCE and different time intervals of 20, 30, and 60 min.

2.2.3 Thermal Oxidation. Titanium alloy was oxidized by heating in a furnace at 800 °C for 2-h time period. The sample was air cooled to room temperature, and then washed with acetone, followed by drying, and the sample was then soaked in Hank solution for various time intervals from 1 to 20 h. Corrosion tests were performed immediately after soaking, in freshly prepared Hank solution.

3. Results and Discussion

The chemical composition of the alloy is given in Table 10, and the optical microstructure of the sample are given in Fig. 21. The microstructure clearly reveals α and β phases.

A comparison between potentiodynamic curves of Ti alloy and 316L steel shows that the Ti alloy is superior to steel regarding passivity and corrosion resistance property (Fig. 1 and Table 1). It is also seen from the cyclic polarization study (Fig. 2) that the curve for stainless steel, after backward

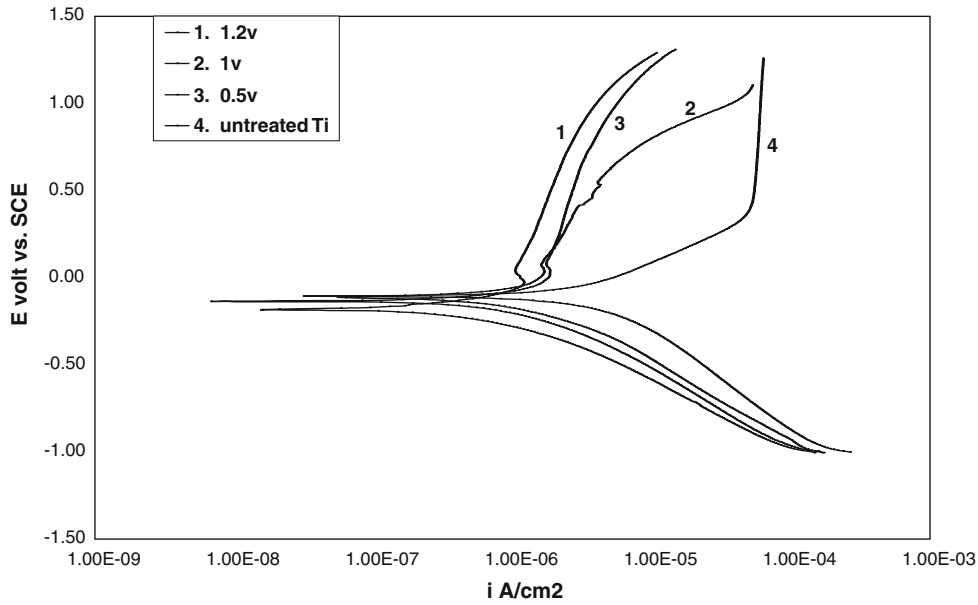

Fig. 5 Potentiodynamic curves in Hank solution after surface treatment of passivation in Hank solution for 20 min at various potential

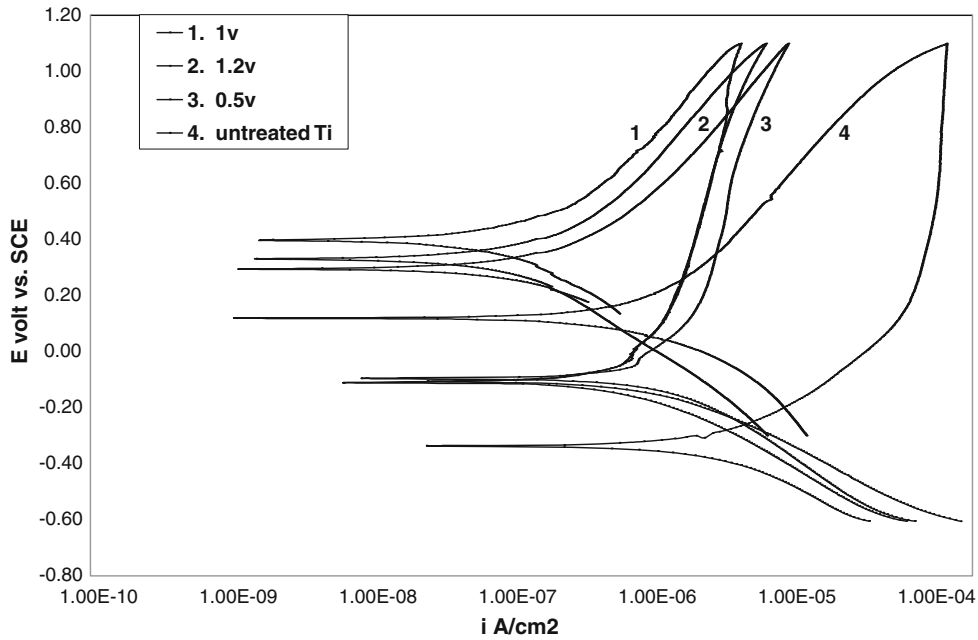

Fig. 6 Cyclic polarization curves in Hank solution after surface treatment of passivation in Hank solution for 20 min at various potential

scanning, moves clockwise. The backward scan curve cuts the passivity region at *Re-passivity potential* or *Protection potential*. In contrast, the curve for the Ti alloy, on reverse scanning, changes to anti-clockwise direction as shown by the arrow in the figure. This reflects that Ti alloy is having better corrosion resistance to pitting compared to that of 316L steel. It is also to be noted that the difference between anodic-cathodic transition potential and the E_{corr}, for the Ti alloy, is greater compared to that for stainless steel.

3.1 Effect of Anodization

The first thing to be noticed in the polarization curves of the anodized samples (Fig. 3) is that the corrosion potentials of the anodized samples have become nobler compared to that of untreated one. The corrosion rates of some of the curves (Fig. 3, curves 1 and 2) are showing lower current values than those shown by the corrosion rates of the untreated ones. The sample anodized at 16 V is showing minimum corrosion rate and passive current density (curve 1), while the untreated sample is showing maximum corrosion rate (Table 2) and passive current density.

From the cyclic polarization curve of the same anodized sample (Fig. 4), it is seen that all the curves during reverse scan are showing lower current, making the surface more passive. It is seen that the untreated sample is showing very big hysteresis area, and in comparison, the hysteresis areas of all the treated samples are less, and the anodization at 16 V (curve 1) is

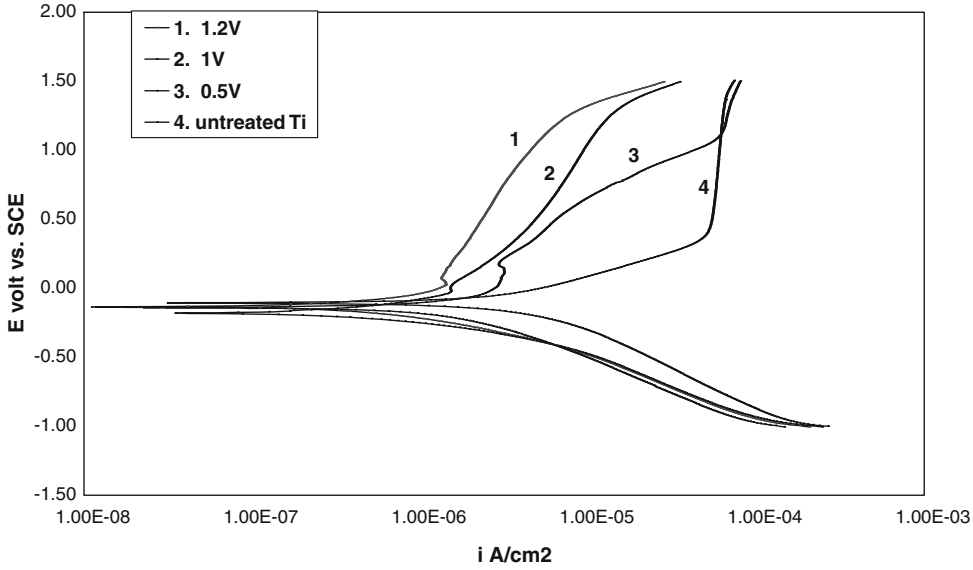

Fig. 7 Potentiodynamic curves in Hank solution after surface treatment of passivation in Hank solution for 30 min at various potential

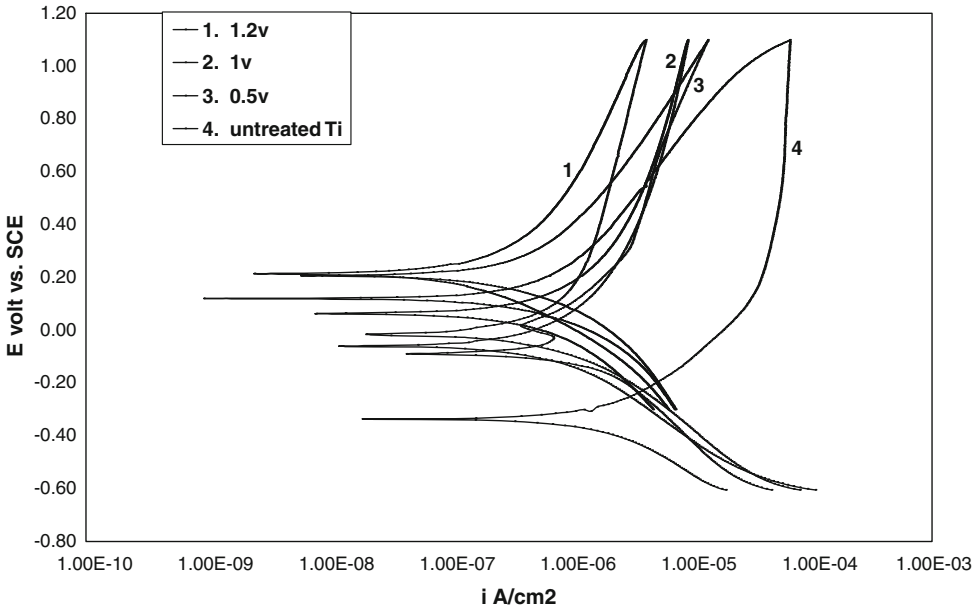

Fig. 8 Cyclic polarization in Hank solution after surface treatment of passivation in Hank solution for 30 min at various potential

showing minimum hysteresis area and the highest corrosion resistance. Larger the hysteresis area, the greater the disruption of surface passivity and the more the difficulty in restoring passivity, leading to greater risk of localized corrosion. Lower current in the reverse scan indicates that the surface is more passive whereas higher current in reverse scan is caused by decreasing passivity, indicating initiation of localized corrosion (pitting or crevice corrosion).

3.2 Effect of Passivation

Potentiodynamic curves of passivation treatments for Ti specimen at different potentials for 20-min time interval are depicted in Fig. 5. It is seen that the curve passivated at 1.2 V gives lower corrosion rate than those at 1 V, 0.5 V, and for

Table 3 E_{corr} and I_{corr} values of Ti alloy in Hank solution after surface treatment by passivation in Hank solution

Sample	E_{corr}, mV vs. SCE	I_{corr}, μA/cm^2
0.5 V 20 min	−155.3	1.252
0.5 V 30 min	−155.3	1.583
0.5 V 60 min	19.42	1.099
1 V 20 min	−155.3	0.803
1 V 30 min	−155.3	1.070
1 V 60 min	−419.9	0.984
1.2 V 20 min	−211.2	0.778
1.2 V 30 min	−116.5	0.665
1.2 V 60 min	−194.2	0.494

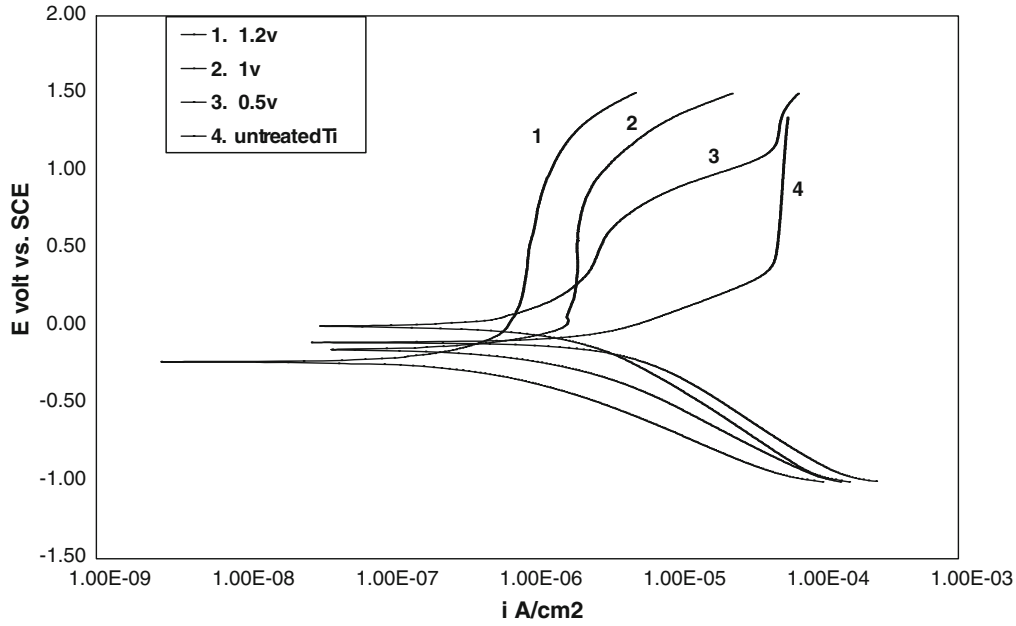

Fig. 9 Potentiodynamic curves in Hank solution after surface treatment of passivation in Hank solution for 1 h at various potential

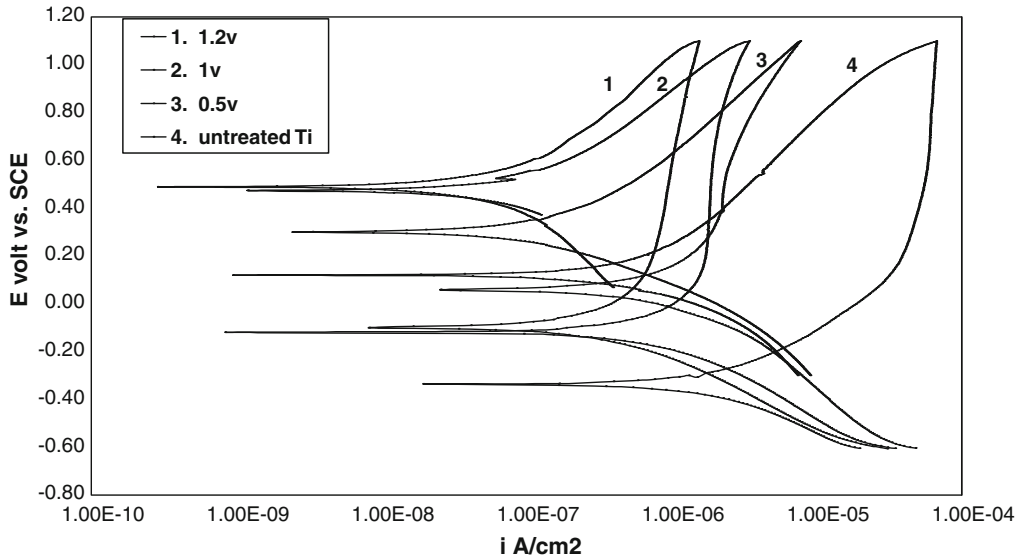

Fig. 10 Cyclic polarization curves in Hank solution after surface treatment of passivation in Hank solution for 1 h at various potential

untreated Ti sample. It is also seen from the corresponding cyclic polarization curves (Fig. 6) that the hysteresis areas of passivated samples are less than that of untreated sample. Similar effects of corrosion rates (Fig. 7, 9) and cyclic polarizations (Fig. 8, 10) were found when the duration of passivation was increased from 20 to 30 min, and finally to 60 min (Table 3). It is found that longer the duration of passivation, the better the corrosion-resistant material produced.

3.3 Effect of Thermal Oxidation and Subsequent Soaking in Hank Solution

It is seen that the corrosion rate can be brought down by thermal oxidation and soaking in Hank solution for different durations of time (Fig. 11 and Table 4), and passive current density is also reduced with this treatment, as seen from cyclic polarization (Fig. 12). The hysteresis areas are also found to be drastically reduced by this treatment, indicating better corrosion resistance film formation. Duration time of

Table 4 E_{corr} and I_{corr} values of Ti alloy in Hank solution after surface treatment of 2 h of furnace heating at 800 °C and then exposure in Hank solution for different time intervals

Sample	E_{corr}, mV vs. SCE	I_{corr}, μA/cm^2
2 h f/c heat + 2 h exposure	−197.7	1.746
2 h f/c heat + 4 h exposure	−314.0	0.953
2 h f/c heat + 20 h exposure	−209.3	1.898

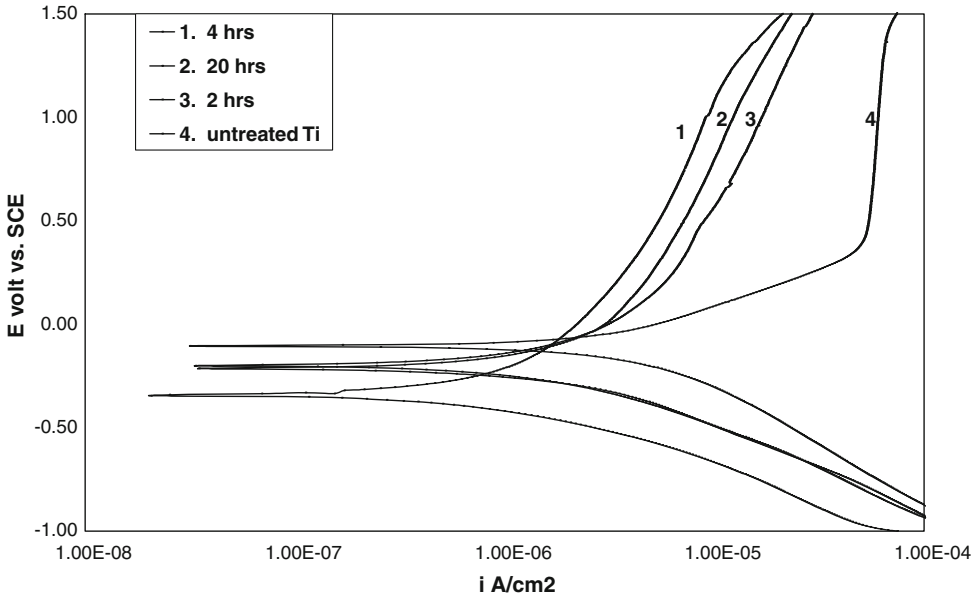

Fig. 11 Potentiodynamic curves in Hank solution after 2 h of furnace heating and then soaking in Hank solution for different time intervals

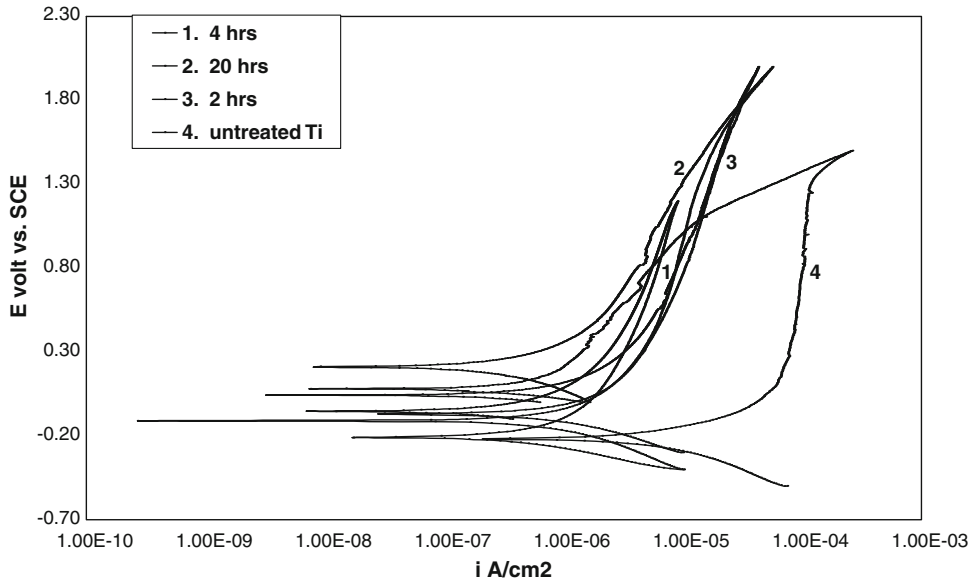

Fig. 12 Cyclic polarization curves in Hank solution after 2 h of furnace heating and then soaking in Hank solution for different time intervals

soaking is also significant as the optimum time is found to be 4 h with the minimum values of corrosion rate and passive current density.

3.4 Comparison of Corrosion Behavior for Different Surface Treatments

Table 5 and Fig. 13 display the comparative results of corrosion behavior of the Ti alloy and the effects of surface treatments. It clearly indicates that all the surface treatments produced an enhanced corrosion resistance property compared to that of an untreated one. While anodization treatment in phosphoric acid at 16 V with 30 min gave minimum corrosion rate, the treatment of passivation as well as thermal oxidation followed by prolonged soaking in Hank solution also have been quite successful in producing highly corrosion-resistant implant material.

Table 5 Comparative results of corrosion behavior of the titanium alloy and effects of surface treatments

Sample	I_{corr}, μA/cm^2
Anodization at 7 V 30 min	3.819
Anodization at 13 V 30 min	1.319
Anodization at 16 V 30 min	0.051
Anodization at 25 V 30 min	1.802
Passivated at 0.5 V 20 min	1.252
Passivated at 0.5 V 30 min	1.583
Passivated at 0.5 V 60 min	1.099
Passivated at 1 V 20 min	0.803
Passivated at 1 V 30 min	1.07
Passivated at 1 V 60 min	0.984
Passivated at 1.2 V 20 min	0.778
Passivated at 1.2 V 30 min	0.665
Passivated at 1.2 V 60 min	0.494
Oxidation 2 h f/c heat + 2 h exposure	1.746
Oxidation 2 h f/c heat + 4 h exposure	0.953
Oxidation 2 h f/c heat + 20 h exposure	1.898
Untreated sample	4.225

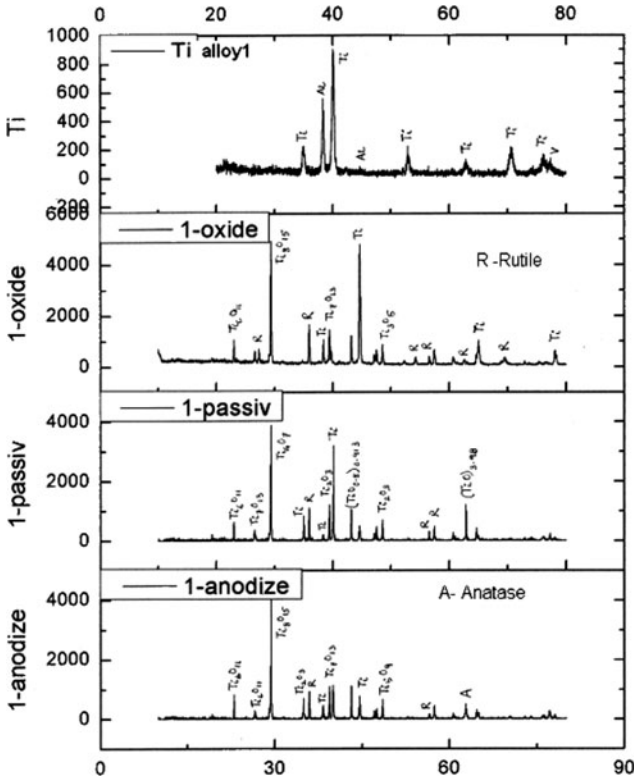

Fig. 14 XRD of Ti alloy before and after various surface treatments

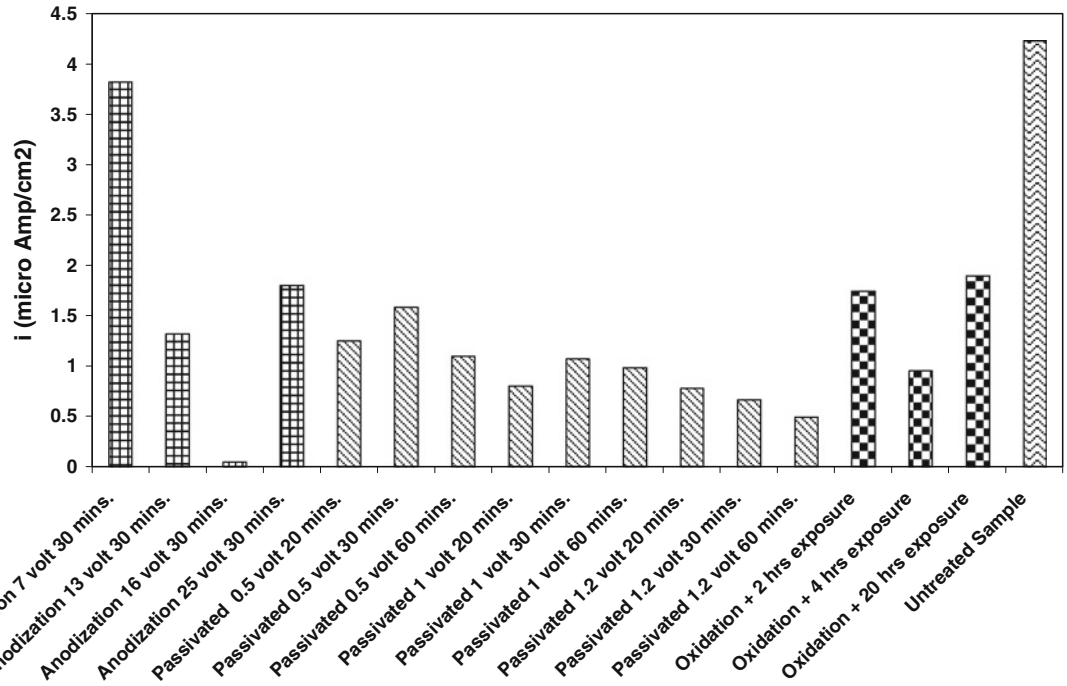

Fig. 13 Comparative results of corrosion rates of the titanium alloy and effects of surface treatments

Implant materials used for hip joint need to have good fatigue strength. In general, fatigue strength of an alloy with thick oxide coating is lower than that without coating. However, it depends a lot on the type of coating film formed. If there are many microcracks in the coating of the material under tensile stress, as found in hard anodized coating, then the fatigue strength will decrease. The presence of the compressive residual internal stress within the coatings gives improved performance in fatigue properties, whereas the development of the tensile residual internal stress within the substrate may cause an early crack initiation in the substrate adjacent to the coating. In this investigation, though the surface characteristics of the coating has not been studied, it is thought much of the microcracks generated have been healed through prolonged soaking in Hank solution. Reduction of hysteresis areas by this treatment (Fig. 12) indicates the formation of nonporous and better corrosion-resistant surface film with minimum microcracks.

3.5 XRD Study

Figure 14 displays the XRD of surface-treated and untreated titanium alloy. It is seen that the peaks for the presence of aluminum, titanium, and vanadium have been obtained in alloy without any treatment, while peaks for various kinds of oxides including rutile are found for all the surface-treated samples. In case of passivation, a number of various oxide layers are formed, while in anodization, in addition to those oxides, anatase is also formed. The presence of anatase, along with other oxides and the absence of any Ti phase on the surface in the XRD analysis may be the reason for lower corrosion rates (Fig. 13) compared to other treatments.

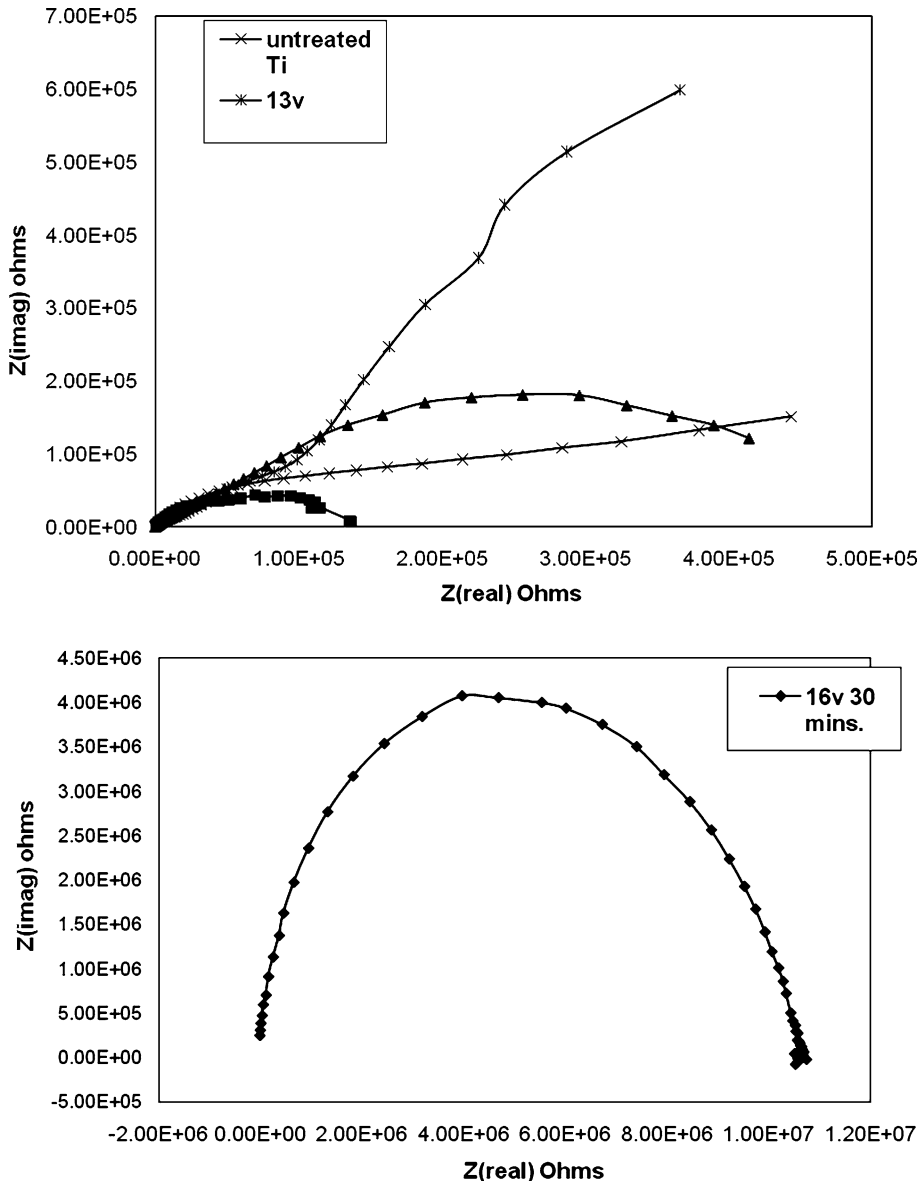

Fig. 15 Potentiostatic EIS data of Nyquist plot of Ti in Hank solution after surface treatment of anodization in phosphoric acid at different potentials

3.6 Electrochemical Impedance Spectroscopy Study

For a better understanding of the fundamental aspects of corrosion phenomenon of a metallic system in an aqueous corrosive environment, EIS study has been carried out.

The phenomenon occurring at the interface of the solid metal-electrolyte is a complex process consisting of line of positively and negatively charged ions which can be represented by an equivalent AC electrical circuits, consisting of capacitances due to double layers and coatings or film formation on the surfaces, polarization resistances, pore resistances, and various impedances due to, diffusion of ions, movement of charge into and away from the metal surface, and adsorption of cations and anions. This phenomenon occurring at the interface can be interpreted from Nyquist and Bode plots which have been depicted and discussed in the later sections for various surface treatments.

3.6.1 Effect of Anodization. Figure 15 displays the Nyquist plot of Ti alloy anodized in 0.3 M phosphoric acid for 30 min at different potentials. It can be seen that the curve for 13 V shows the characteristics of Randle with Warburg resistance. The curves for 7 V and 25 V, both show the characteristics of Randle circuit. However, for 7 V the R_p value is lower than that for 25 V, indicating anodization at 25 V produces a higher corrosion resistance than that at 7 V. This is supported by the potentiodynamic curve (Fig. 3). The curve for 16 V anodization (shown separately at the bottom of Fig. 15),

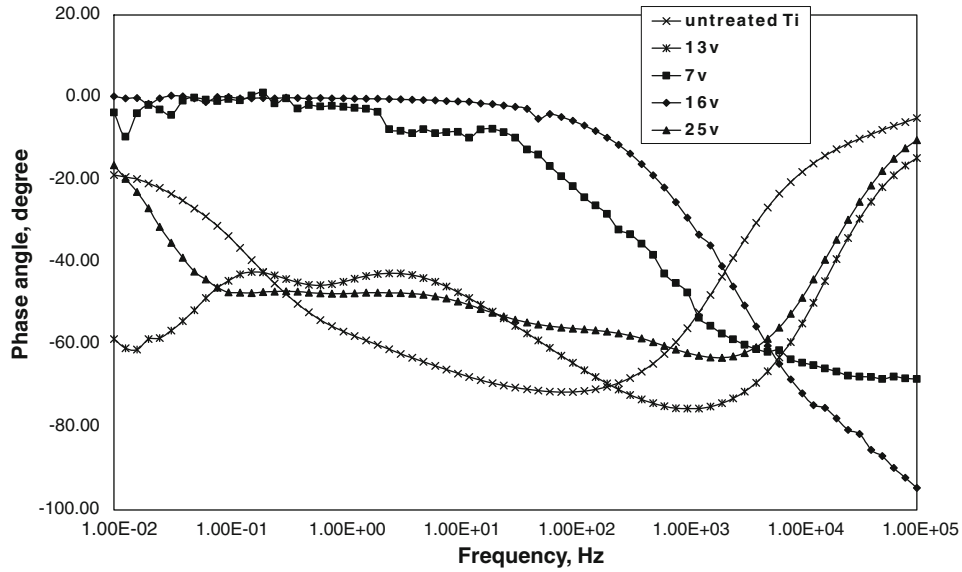

Fig. 16 Potentiostatic EIS data of Bode plot of Ti in Hank solution after surface treatment of anodization in phosphoric acid at different potentials

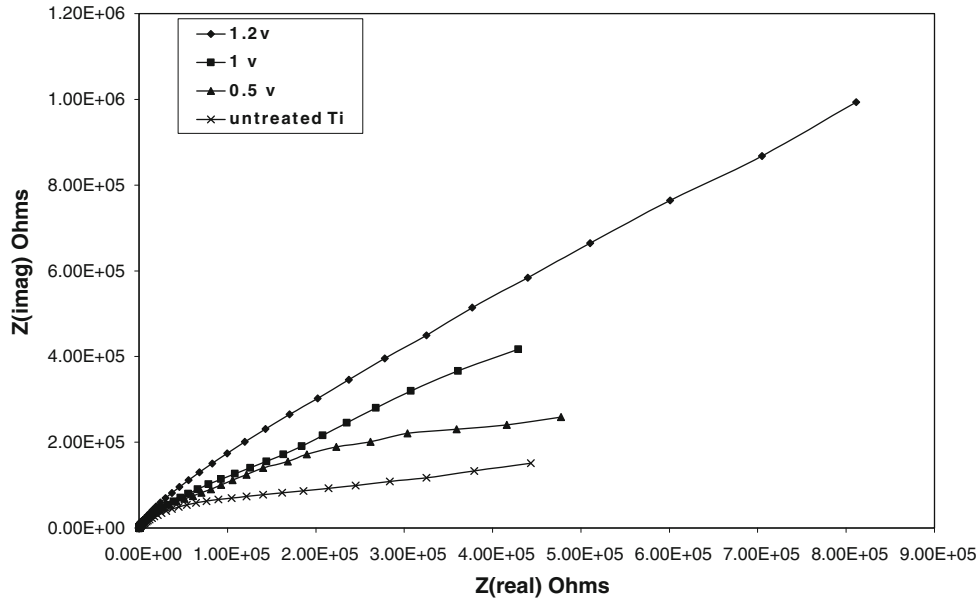

Fig. 17 Potentiostatic EIS Nyquist plot of Ti in Hank solution after surface treatment of passivation in Hank solution for 1 h at different potentials

shows the characteristics of the coating circuit, with R_p value higher than all other curves. From the Bode plot (Fig. 16), it is seen that the curve anodized at 13 V is more or less giving the characteristics of Mixed Control circuit.

3.6.2 Effect of Passivation. It is seen from the Nyquist plots that all the curves show the characteristics of Randle circuit with Warburg resistance (Fig. 17), while the Bode plot (Fig. 18) shows, all of the curves approach up to -80^o phase angle at mid-range frequency, indicating existence of capacitances, along with polarization resistance. The characteristic of the curve in Bode plot seems to represent double layered capacitance with Warburg resistance, but the same cannot be clearly predicted from Nyquist plot. However, it is very much reflected from the highest $Z_{(imag)}$ as well as R_p, that the passivation treatment at 1.2 V produced very good passive film of high resistance to pitting corrosion.

3.6.3 Effect of Thermal Oxidation, Followed by Soaking in Hank Solution. Figure 19 displays Nyquist plot for the alloy heated for 2 h at 800 °C and then exposed in Hank solution for different time intervals, and Fig. 20 shows the corresponding bode plot. All the curves of both the Nyquist and the bode plots seem to follow the characteristics of Randle with Warburg resistance. It is to be noted that both $Z_{(imag)}$ and R_p values for 4-h exposure are the highest, indicating the formation

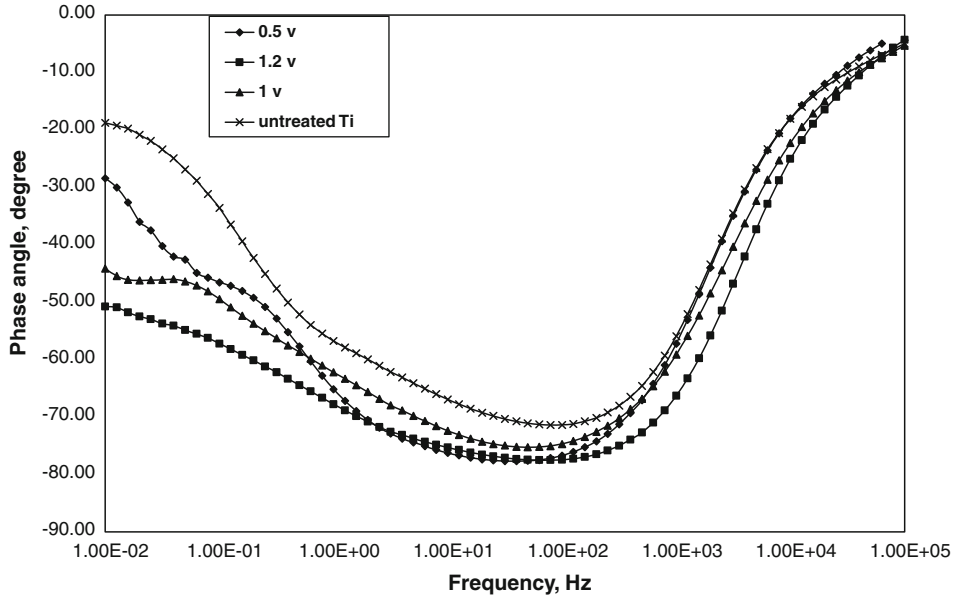

Fig. 18 Potentiostatic EIS data of Bode plot of Ti in Hank solution after surface treatment of passivation in Hank solution for 1 h at different potentials

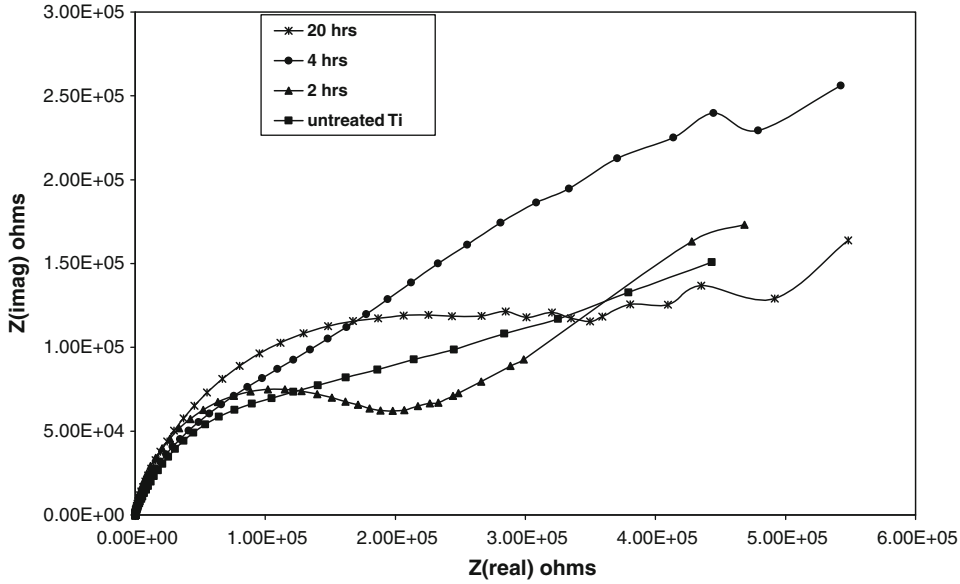

Fig. 19 Potentiostatic EIS data of Nyquist plot of Ti in Hank solution after 2 h of furnace heating at 800 °C and then exposure in Hank solution for different time intervals

of high corrosion-resistant oxide coating. This fact is supported by the polarization curve (Fig. 11), showing minimum corrosion current and passive current density (Fig. 12) for this treatment.

3.6.4 Determination of EIS Parameters (R_p, R_s, C_{dl}, Y_o, W_d). Determination of EIS parameters by finding out the most suitable electrical R-L-C circuit from the Nyquist and bode plot is complicated process. In reality there are much deviations from ideal cases of equivalent circuits given in literature. Several electrochemical phenomena occurring at the metal electrolyte interface lead to more number of equivalent electrical circuits, consisting of capacitances, resistances, and some inductances, than what can be designed and made tp fit with the built-in software. In this investigation, EIS parameters have been computed with best matching circuit from the experimental data. These have been depicted in Table 6-8.

It is seen from the Table 6, that the polarization resistance value for 16-V anodization is much higher and the capacitance value (C_f) which is equivalent to Y_o, is much lower than for the other curves. This makes the 16-V anodization the best among the other anodized samples. For passivation treatment (Table 7), it is seen that 1.2 V gives the highest corrosion resistance (R_p) and lower CPE (Y_o) than that for 0.5 and 1 V, for

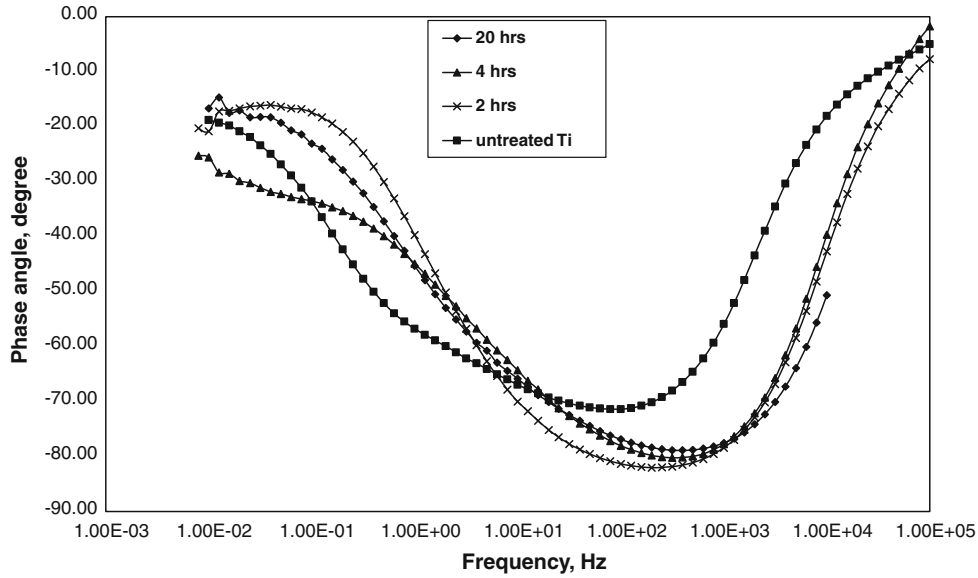

Fig. 20 Potentiostatic EIS data of Bode plot of Ti in Hank solution after 2 h of furnace heating at 800 °C and then exposure in Hank solution for different time intervals

Table 6 EIS data of Ti alloy anodized with 0.3 M phosphoric acid

Sample	R_p, ohms	Y_o, F	Alpha	W_d, ohms	C_f, F
Ti alloy anodization 7 V 30 min	1.13E+05	2.81E−08	7.51E−01	1.44E−03	…
Ti alloy anodization 13 V 30 min	8.87E+03	5.32E−07	9.15E−01	7.76E−06	…
Ti alloy anodization 16 V 30 min	1.02E+07	…	…	…	7.41E−12
Ti alloy anodization 25 V 30 min	5.65E+05	5.54E−06	6.35E−01	…	…
Untreated Ti alloy	1.74E+05	6.07E−06	8.03E−01	2.22E−05	

Table 7 EIS data of Ti alloy passivated in Hank solution varying voltage and time

Sample	R_p, ohms	Y_o, F	Alpha	W_d, ohms
Ti alloy passivation 0.5 V 20 min	1.38E+05	3.58E−06	8.53E−01	3.57E−06
Ti alloy passivation 1 V 20 min	9.91E+03	4.20E−06	8.81E−01	4.05E−06
Ti alloy passivation 1.2 V 20 min	2.34E+05	5.32E−06	8.54E−01	7.30E−06
Ti alloy passivation 0.5 V 30 min	2.40E+05	5.42E−06	8.40E−01	2.87E−05
Ti alloy passivation 1 V 30 min	4.03E+05	5.02E−06	8.26E−01	1.76E−05
Ti alloy passivation 1.2 V 30 min	4.74E+04	2.86E−06	9.03E−01	4.61E−06
Ti alloy passivation 0.5 V 60 min	1.31E+05	4.38E−06	8.83E−01	9.13E−06
Ti alloy passivation 1 V 60 min	9.80E+04	4.35E−06	8.52E−01	6.55E−06
Ti alloy passivation 1.2 V 60 min	1.21E+05	2.56E−06	8.85E−01	2.59E−06

60-min time duration. Same can be concluded for 20- and 30-min passivation after considering the combined effect of all the EIS parameters. This goes in accordance with the results from polarization curves and results (Fig. 5, 7, 9 and Table 5). For thermal oxidation and subsequent soaking in Hank solution (Table 8), the 4-h exposure gives maximum polarization as well as warburg resistance and hence produces high corrosion resistance surface.

Thus resistance to localized corrosion for Ti alloy implant can be improved to a great extent by surface treatments, due to formation of highly corrosion-resistant film which causes the enhancement of capacitive and resistive impedances. Corrosion rate of the material depends on polarization resistance if it is an activation polarization controlled reaction, but with formation of oxide coating, anodized or passive films, the rate of corrosion is also controlled by various capacitance or constant phase elements and warburg resistances. Therefore, besides polarization values R_p, other EIS parameters need to be considered while determining the most corrosion-resistant implant material.

Besides pitting, implant material is also susceptible to crevice and fretting corrosions. Surface treatments that produce strong protective passive film with good capability of repassivation can retard the propagation of both fretting and crevice forms of corrosion as well. A crevice initiated at a site may stop growing if it is repassivated, in a well-surface-treated implant material. Fretting corrosion which is the conjoint action of mechanical wear and corrosion, occurs in the implant, when the micromotion between two metals or metal/body fluid, breaks the passivation layers. Points of rupture may be reoxidized under a favorable repassivation potential, helping fretting to discontinue. Hence, studies of characteristic of passivity and passivity breakdown in the form of pitting, also throw light on protectiveness of these surface-treated implant against other forms of localized corrosion.

4. Conclusion

Surface modification of Ti-alloy by anodization, passivation, and thermal oxidation is very effective in producing implant material with high resistance to localized corrosion in artificial physiological solution. It produced high corrosion resistance surface films, consisting of various types of oxides along with anatase and rutile as evident from drastically reduced corrosion current, low passive current density and narrower hysteresis areas of cyclic polarization curves, high impedance, polarization, and warburg resistance and lower capacitance.

Appendix

See Fig. 21 and Table 9 and 10.

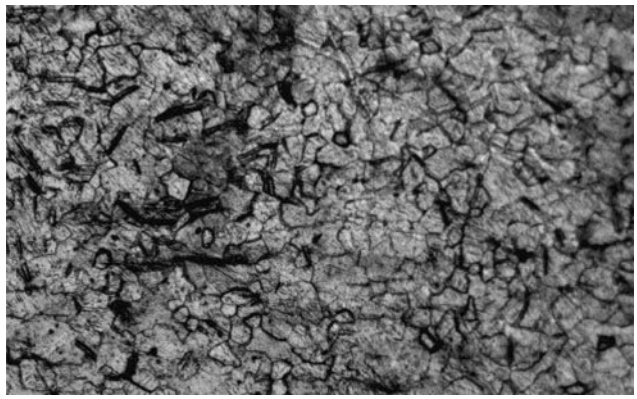

Fig. 21 Optical microstructure of (Ti-6Al-4V) annealed at 800 °C in argon atmosphere, Magnificat

Table 8 EIS data of Ti alloy soaked in Hank solution after thermal oxidation treatment

Sample	R_p, ohms	Y_o, F	Alpha	W_d, ohms
Ti alloy furnace heating 2 h + 2 h exposure	1.59E+05	8.46E−07	9.16E−01	1.86E−05
Ti alloy furnace heating 2 h + 4 h exposure	2.97E+05	1.81E−06	8.26E−01	3.12E−0.3
Ti alloy furnace heating 2 h + 20 h exposure	2.43E+05	9.38E−07	8.59E−01	1.26E−05

Table 9 Composition of Hank solution

NaCl, g/L	$MgCl_2$, g/L	$CaCl_2$, g/L	KCl, g/L	KH_2PO_4, g/L	$NaHCO_3$, g/L	Na_2HPO_4, g/L	KH_2PO_4, g/L	Glucose, g/L
8.0	0.2	0.14	0.4	0.06	0.35	0.06	0.06	1.0

Table 10 Chemical composition of the alloy Ti-6Al-4V

N, wt.%	C, wt.%	H, wt.%	Fe, wt.%	O, wt.%	Al, wt.%	V, wt.%	Ti, wt.%
0.048	0.081	0.009	0.315	0.012	5.7	3.6	Balance

References

1. B. Kasemo and J. Lausmaa, Aspect of Surface Physics on Titanium Implants, *Swed. Dent. J.*, 1983, **28**(Suppl.), p 19–36
2. J. Lausmaa and B. Kasemo, Surface Spectroscopic Characterization of Titanium Implant Materials, *Appl. Surf. Sci.*, 1990, **45**, p 133–146
3. I. Olefjord and S. Hansson, Surface Analysis of Four Dental Implant Systems, *Int. J. Oral Maxillofac. Implants*, 1993, **8**, p 32–40
4. G. Rådegran, J. Lausmaa, L. Matsson, U. Rolander, and B. Kasemo, Preparation of Ultra-Thin Oxide Window on Titanium for TEM Analysis, *J. Electron Microsc. Tech.*, 1991, **19**, p 99–106
5. H. Zitter and H.J. Plenk, The Electrochemical Behaviour of Metallic Implant Materials as Indicator of Their Biocompatibility, *J. Biomed. Mater. Res.*, 1987, **21**, p 881–896
6. D.F. Williams, Corrosion of Implant Materials, *Ann. Rev. Mater. Sci.*, 1976, **6**, p 237–265
7. R.J. Solar, S.R. Pollack, and E. Korostoff, In Vitro Corrosion Testing of Titanium Surgical Implant Alloys: An Approach to Understanding Titanium Release from Implants, *J. Biomed. Mater. Res.*, 1979, **13**, p 217–250
8. P. Tengvall and I. Lundström, Physico-Chemical Considerations of Titanium as a Biomaterial, *Clin. Mater.*, 1992, **9**, p 115–134
9. C.B. Johansson, On Tissue Reactions to Metal Implants, Thesis, University of Göteborg, Sweden, 1991
10. S.L. de Assis, S. Wolynec, and I. Costa, Corrosion Characterization of Titanium Alloys by Electrochemical Techniques, *J. Electrochim. Acta*, 2006, **51**, p 1815–1819
11. R. Narayanana and S.K. Seshadri, Phosphoric Acid Anodization of Ti-6Al-4V. Structural and Corrosion Aspects, *J. Corros. Sci.*, 2007, **49**, p 542–558
12. M.H. Wong, F.T. Cheng, and H.C. Man, Characteristics, Apatite-Forming Ability and Corrosion Resistance of NiTi Surface Modified by AC Anodization, *J. Appl. Surf. Sci.*, 2007, **253**, p 7527–7534
13. R. Narayanan and S.K. Seshadri, Synthesis and Corrosion of Functionally Gradient TiO_2 and Hydroxyapatite Coatings on Ti-6Al-4V, *J. Mater. Chem. Phys.*, 2007, **106**, p 406–411
14. J.R. Scully, Polarization Resistance Method for Determination of Instantaneous Corrosion Rates, *Corrosion*, 2000, **56**, p 199
15. ASTM G 5: Potentiostatic and Potentiodynamic Anodic Polarization Measurements
16. ASTM G 59: Polarization Resistance Measurements
17. ASTMG 61: Cyclic Polarization Measurements for Localized Corrosion
18. *DC Electrochemical Test Methods*, N.G. Thompson and J.H. Payer, Ed., (Houston, TX), National Association of Corrosion Engineers